(2)

NAVAL POSTGRADUATE SCHOOL
Monterey, California

THESIS

DEVELOPMENT OF AN
UNMANNED AIR RESEARCH VEHICLE FOR
SUPERMANEUVERABILITY STUDIES

by

Christopher Mark Cleaver

March 1990

Thesis Advisor: Richard Howard
Co-Advisor: James Hauser

Unclassified

Security Classification of this page

REPORT DOCUMENTATION PAGE

1a Report Security Classification: Unclassified	1b Restrictive Markings
2a Security Classification Authority	3 Distribution Availability of Report: Approved for public release; distribution is unlimited.
2b Declassification/Downgrading Schedule	
4 Performing Organization Report Number(s)	5 Monitoring Organization Report Number(s)
6a Name of Performing Organization: Naval Postgraduate School; 6b Office Symbol (*If Applicable*): 67	7a Name of Monitoring Organization: Naval Postgraduate School
6c Address (*city, state, and ZIP code*): Monterey, CA 93943-5000	7b Address (*city, state, and ZIP code*): Monterey, CA 93943-5000
8a Name of Funding/Sponsoring Organization; 8b Office Symbol (*If Applicable*)	9 Procurement Instrument Identification Number
8c Address (*city, state, and ZIP code*)	10 Source of Funding Numbers: Program Element Number; Project No; Task No; Work Unit Accession No

11 Title (*Include Security Classification*): DEVELOPMENT OF AN UNMANNED AIR RESEARCH VEHICLE FOR SUPERMANEUVERABILITY STUDIES

12 Personal Author(s): Cleaver, Christopher M.

13a Type of Report	13b Time Covered	14 Date of Report (*year, month,day*)	15 Page Count
Master's Thesis	From To	1990, March 29	54

16 Supplementary Notation: The views expressed in this thesis are those of the author and do not reflect the official policy or position of the Department of Defense or the U.S. Government.

17 Cosati Codes			18 Subject Terms (*continue on reverse if necessary and identify by block number*)
Field	Group	Subgroup	UAV, RPV, Telemetry, Supermaneuverability, Ducted Fan, Agility

19 Abstract (*continue on reverse if necessary and identify by block number*)

With the advent of all-aspect missiles and highly maneuverable threat aircraft, maintaining air superiority in the future will require innovative solutions to current aerodynamic and propulsive limitations. Unmanned Air Vehicles (UAV's) provide an excellent experimental alternative for supermaneuverability investigations, providing dynamic flight measurements not available in wind tunnels. A 1/8 geometrically scaled F-16A was constructed and test flown in order to provide a proven, highly maneuverable, airframe for control configuration modifications. The aircraft was configured for the measurement of airspeed, angle of attack, sideslip angle, and control surface deflection. A seven-channel telemetry system was designed to transmit the flight measurement data to a ground station for display and recording. Follow-on research will complete the on-board systems and perform a baseline evaluation for comparison with future flight tests with varied control configurations.

20 Distribution/Availability of Abstract	21 Abstract Security Classification
[X] unclassified/unlimited [ ] same as report [ ] DTIC users	Unclassified
22a Name of Responsible Individual: Richard M. Howard	22b Telephone (*Include Area code*): (408) 646-2870; 22c Office Symbol: Code 67Ho

DD FORM 1473, 84 MAR 83 APR edition may be used until exhausted

All other editions are obsolete

security classification of this page: Unclassified

Approved for public release; distribution is unlimited.

Development of an Unmanned Air Research Vehicle for Supermaneuverability Studies

by

Christopher Mark Cleaver
Lieutenant Commander, United States Navy
B.S., United States Naval Academy, 1977

Submitted in partial fulfillment of the requirements
for the degree of

MASTER OF SCIENCE IN AERONAUTICAL ENGINEERING

from the

NAVAL POSTGRADUATE SCHOOL

MARCH 1990

Author: Christopher M. Cleaver
Christopher Mark Cleaver

Approved by: Richard M. Howard
Richard M. Howard, Thesis Advisor

James P. Hauser
James P. Hauser, Second Reader

E. R. Wood
E. Roberts Wood
Chairman, Department of Aeronautics and Astronautics

ABSTRACT

With the advent of all-aspect missiles and highly maneuverable threat aircraft, maintaining air superiority in the future will require innovative solutions to current aerodynamic and propulsive limitations. Unmanned Air Vehicles (UAV's) provide an excellent experimental alternative for supermaneuverability investigations, providing dynamic flight measurements not available in wind tunnels. A 1/8 geometrically scaled F-16A was constructed and test flown in order to provide a proven, highly maneuverable, airframe for control configuration modifications. The aircraft was configured for the measurement of airspeed, angle of attack, sideslip angle, and control surface deflection. A seven-channel telemetry system was designed to transmit the flight measurement data to a ground station for display and recording. Follow-on research will complete the on-board systems and perform a baseline evaluation for comparison with future flight tests with varied control configurations.

TABLE OF CONTENTS

LIST OF FIGURES

ACKNOWLEDGEMENTS

There were many people involved in this project who without their help and guidance would have made it more difficult. I'd like to thank the Polo field group, Pat Hickey, Don Harvey, and Al McGuire, for their assistance during the construction of the F-16. Don Meeks, with his vast experience with model building, provided many ideas and solutions to the big and small things that are often overlooked. Without the help of Mike Callaway, this project would never have "launched." His experience and knowledge of ducted-fan models proved to be invaluable. I must also thank his wife Diane for allowing him to come play during the final stages of her pregnancy.

Most of all, I would like to thank Dr. Rick Howard and Dr. Jim Hauser for their patience, guidance, enthusiasm, and long hours during the tenure of the project. Without them I would still be gluing and soldering.

I. INTRODUCTION

The outcome of a visual air-to-air engagement depends to a large part on the initial conditions of the event. The goal when starting from an offensive scenario is to maneuver the aircraft to a position in order to fire a weapon. The maneuvers required when in a defensive position, on the other hand, take on a more radical nature, since the goal is a matter of pure survival rather than achieving a weapons solution. The more "agile" an aircraft, the greater the chances are of obtaining the desired outcome, given equal pilot ability and visual contact between aircraft.

Agility, in an aircraft performance context, has been defined by some as a scientific term which identifies a unique characteristic of aircraft dynamics. It is frequently associated with such concepts as controllability, maneuverability, pointing ability, acceleration, flight dynamics, and flying qualities. The development of an agile fighter requires consideration of many elements, such as the threat, available technology, and tactics. Figure 1. identifies some of the inputs necessary for a new design. [Ref. 1:p. 1]

Maintaining air superiority in the future will depend upon the agility of an aircraft, especially in a high angle-of-attack (alpha) flight regime. This demand for agility will result in intentional flight at high alpha in order to generate the angular accelerations and positional maneuver advantages required for a successful engagement [Ref. 2:p. 3-2]. The fighter can then generate a positional advantage in order to get the first missile shot ("point and shoot" tactic).

Four key technologies are involved in the development of future fighter aircraft.

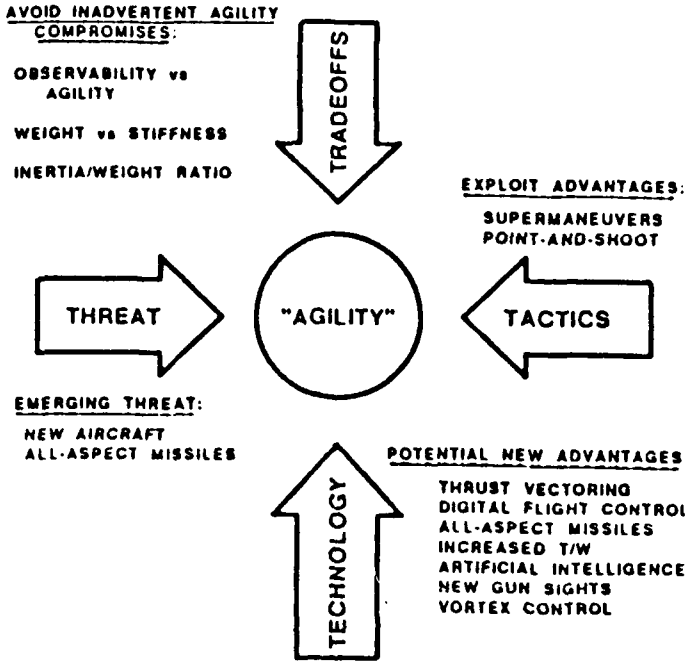

Figure 1. Design Considerations of an "Agile" Fighter [Ref. 1:p. 1]

A. DIGITAL FLY-BY-WIRE CONTROL

Digital fly-by-wire control allows control surfaces to move according to a commanded flight condition rather than a control stick displacement, as with a mechanical system. Digital systems can also provide basic stability for an aircraft that is designed to be marginally stable, or unstable, due to the desire for improved maneuverability. [Ref. 3:p. 561-562] Due to the complex control laws involved with integrated flight controls and vectored thrust, programming flexibility (inherent in digital flight control computers) is of prime importance for the basic system and when modifications are required.

B. DELTA WING/CLOSE-COUPLED CANARD CONFIGURATION

The tailless delta wing configuration takes more advantage from configuration control vehicle (CCV) technology than other wing configurations. With flaps designed to deflect in accordance with a commanded flight condition, several performance advantages result [Ref. 3:p. 562-563]:

- Maximum lift coefficients are improved due to vortex lift
- A properly designed CCV delta wing reduces the angle-of-attack in a high-lift configuration, which permits exploitation of the lift potential more efficiently for takeoff and landing
- Less induced drag at any flap setting, which improves basic maneuvering
- Faster and more precise response to control inputs

A delta wing/close-coupled canard configuration improves maximum lift with fewer penalties than with a long-coupled canard wing. Moving a canard longitudinally forward and downward reduces maximum lift increments as well as increases the minimum drag [Ref. 12:p. 90-91]. The canard system also provides additional control while optimizing lift to drag throughout the flight envelope. [Ref. 3:p. 562-563]

C. SUPERMANEUVERABILITY / VECTORED THRUST

The concept of supermaneuverability encompasses post-stall (high alpha) maneuvering in conjunction with two-dimensional vectored thrust. Pitch and yaw control at high alpha is accomplished by means of the vectored thrust. The aircraft therefore has the capability to pitch and yaw independently of the flight path. [Ref. 3:p. 564]

D. VORTEX CONTROL

Another emerging concept involves strake-generated vortex interactions, which improves maneuverability using non-linear lift generated by a strake. The

interaction of the vortex with the airflow over the wing allows aircraft controllability above an angle of attack at which a conventional wing would have stalled [Ref. 4:p. 289]. The concept of actuated forebody strakes for yaw control at high alpha is also being investigated. Yaw control with rudder becomes less effective at high angles of attack due to the blanking effect of the stalled wing. However, the forebody remains in undisturbed flow and is capable of producing powerful vortex flow fields at high angles of attack. Asymmetrical vortex control is feasible with actuated forebody strakes which provide yaw control by means of a force-moment arm couple [Ref. 5:p. 279-280].

One method of demonstrating advanced technologies is through use of unmanned air vehicles (UAV's), or remotely piloted vehicles (RPV's). Proven airframe designs, such as the F/A-18 and F-16, can be modified to accommodate configuration changes, or entirely new designs, such as the HiMAT aircraft and X-29A, can be utilized. The use of UAV's has the following advantages [Ref. 6:p. 9]:

- Actual dynamic flight measurements
- Inexpensive when compared to a manned research vehicle
- Full integration of aircraft systems not required
- No risk to test pilot
- Small scale airframe easier to modify

Several experiments involving UAV's have provided valuable information. Perhaps the most ambitious endeavor was the highly maneuverable aircraft technology (HiMAT) program undertaken by the Rockwell Corporation in conjunction with NASA (see Figure 2). The goal was to combine advanced technologies, such as aeroelastic tailoring, a close-coupled canard, and relaxed

static stability, to exploit favorable interaction between these technologies and thereby achieve a dramatic improvement in maneuvering performance. Table 1 provides a research data assessment of the program [Ref. 6:p. 2].

The use of RPV's, scaled from current fighter aircraft, takes advantage of proven aerodynamic designs and allows for airframe and flight control modifications to explore new configurations. The NASA Dryden Flight Research Center conducted flight tests of a 3/8-scale F-15 model (Figure 3). The project was designed to investigate controllability at high angles of attack to determine spin modes, to develop spin entry and recovery techniques, and to evaluate the remotely piloted aircraft test method. The results of the study indicated satisfactory correlation with predicted departure/spin criteria. The project further demonstrated that the use of a large-scale model aircraft was valuable for obtaining rapid, dynamic flight data over a wide range of flight conditions. [Ref. 7:p. 2, 31-31]

Prior to the first manned flight, a 22% scaled replica of the forward swept X-29A (Figure 4) was used to verify wind tunnel predicted wing rock at angles of attack above 20°. The model was dropped from a helicopter, flown through a series of test maneuvers, and recovered with a parachute. Air data, flight control deflections, and aircraft response to control inputs were transmitted to a ground station recorder for later analysis. The tests proved to be a successful method of understanding dynamic characteristics of the X-29A since dynamic flight data were gathered in the study. [Ref. 8:p. 1]

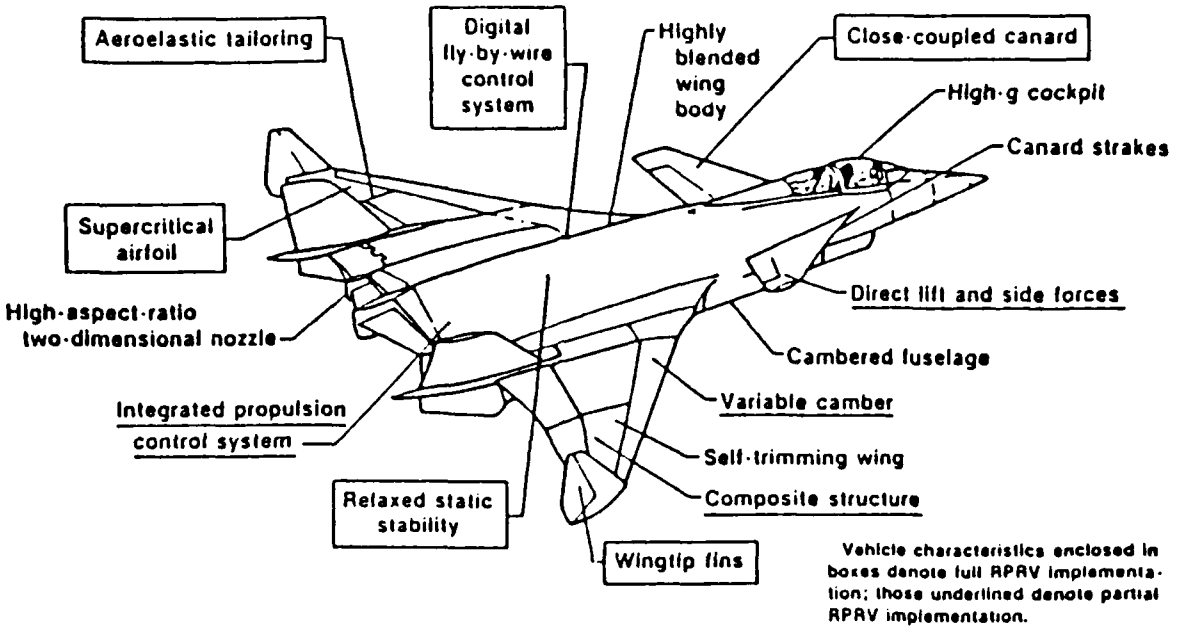

Figure 2. HiMAT Remotely Piloted Research Vehicle [Ref. 6:p. 12]

TABLE 1. DATA ASSESSMENT OF HiMAT PROGRAM [Ref. 6:p. 11]

Technology area	Data quantity	Data quality	Overall assessment
Aerodynamics			
Pressure distributions[a]	Adequate	Excellent	Excellent
Specific excess power	Marginal	Good	Fair
Buffet	Adequate	Fair	Fair
Structures			
Loads on composite structure[a]	Marginal	Excellent	Very good
Deflections and twist[a]	Marginal	Excellent	Very good
Controls			
Stability and control	Adequate	Good	Good
Relaxed static stability	Marginal	Good	Fair
Digital fly-by-wire	Adequate	Excellent	Excellent
Propulsion controls	Marginal	Good	Good

[a]Primary experiments

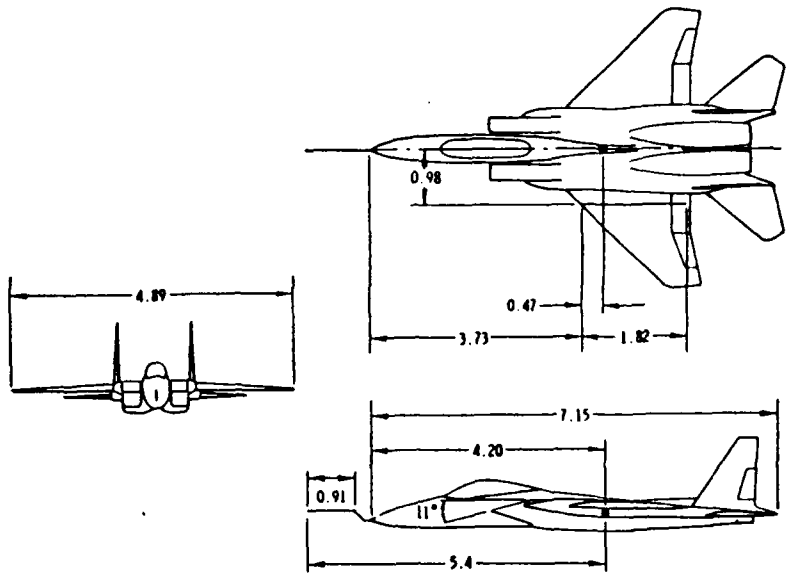

Figure 3. 3/8 Scale F-15. Measurements in meters [Ref. 7:p. 40]

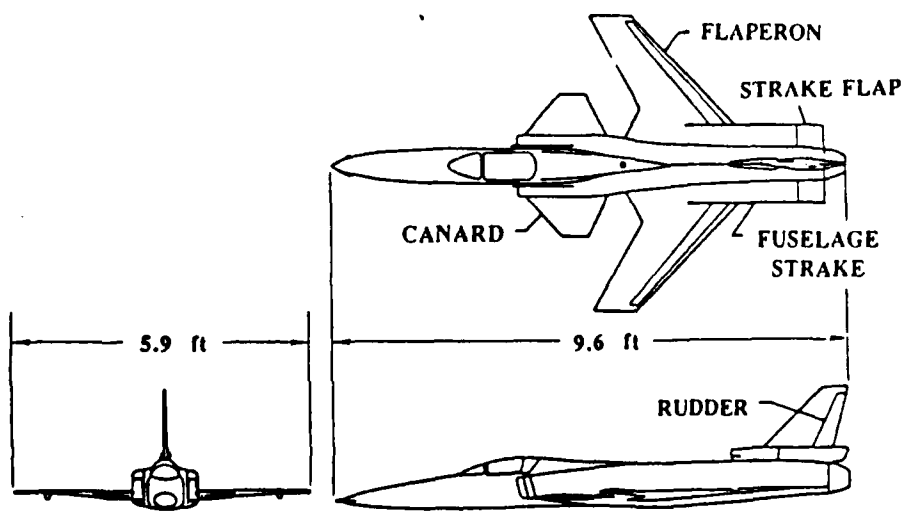

Figure 4. 22% Scale X-29A [Ref. 8:p. 13]

II. SCOPE

An Unmanned Air Vehicle (UAV) flight research program is developing at the Naval Postgraduate School. Sponsored by the Unmanned Aerial Vehicle Joint Project Office (UAV JPO) and AIR-931 (Aircraft Research and Technology) of the Naval Air Systems Command (NAVAIR), the program encompasses engineering, design, and flight test support for UAV and future aircraft systems in research areas of aerodynamics, air vehicle performance, propulsion, stability and control, avionics, and sensor technology.

The full scale General Dynamics F-16A has proven itself to be an effective fighter in its standard configuration, as well as in advanced configurations such as the F-16XL and the F-16 Advanced Fighter Technology Integration (AFTI). A 1/8-scale model of the F-16A, in a full-scale control configuration, serves as an initial test vehicle for supermaneuverability analysis. Due to the relatively small scale of the UAV and the use of commercially available radio control equipment, the scope of the study is limited to varied control configurations, rather than advanced propulsion systems or complex digital fly-by-wire flight control systems. Though scaled geometrically, the model does not have the advantage of being dynamically scaled (mass, moment of inertia, linear/angular velocities and accelerations). The aircraft therefore is not expected to have the same flight characteristics as the full-scale F-16A.

In order to explore new control configurations and their resultant performance characteristics, dynamic measurements are often required that are not obtainable in wind tunnels. A seven-channel telemetry package, consisting of a commercially-developed airborne encoder/transmitter and ground-based

receiver/decoder, was designed to monitor selected parameters that allow for an effective evaluation of a given configuration. Inputs to the F-16A model telemetry system consist of flight control deflections (ailerons, stabilator, and rudder), airspeed, angle-of-attack (alpha), yaw angle (beta), and the airborne radio control system battery voltage reference.

Flight control servo actuator output voltages will be used as a direct input to the telemetry package. A square tipped 1-3/4 inch propeller will be used for airspeed measurement. A parallel Cadmium-Sulfide (CdS) photo sensor, facing the rear of the propeller, provides RPM information to a custom-designed circuit that converts the RPM to a voltage. The airspeed indicator is designed to operate in a range from 19 to 184 mph. Angle-of-attack and yaw-angle voltage inputs will be obtained from low torque potentiometers connected to external vanes.

The ground-based station will consist of a panel of analog meters, as well as a seven-channel data recorder. The analog meters, which provide real time feedback to the flight test engineer, will be scaled for respective units: degrees for control surface deflection and alpha/beta, feet per second for airspeed, and volts for battery output. The ground station panel will also be recorded with a VCR camera during the flight, with verbal commentary describing the maneuvers. The data recorder will be used to record the flight performance parameters for later analysis on data strip charts.

The scope of the initial study consisted primarily of a "proof of concept" for the F-16A model / telemetry system in a standard configuration. Future studies will allow for configuration changes, such as close-coupled canards, nose strakes, and aerodynamic tailoring, in order to analyze the effect on enhanced maneuverability.

III. EXPERIMENTAL EQUIPMENT

A. FLIGHT TEST VEHICLE

The flight test vehicle used for the experiment is a radio controlled 1/8-scale model of the General Dynamics F-16A (Figure 5). The aircraft is composed of a pre-formed lightweight fiberglass fuselage and high density foam wings, rudder, and stabilator. The fuselage is painted with an grey epoxy paint while the foam components were covered with mylar film. Structural support for the fuselage was provided by two 1/4 inch plywood formers, the forward former acting as engine/ducted fan support (Figure 6). The aircraft was also configured with pneumatic retractable landing gear, though the main gear wheels remained exposed approximately one inch. The ducted fan utilizes air from the normal intake as well as from an 80 square inch "cheater hole" located on the bottom of the aircraft. Due to the blockage factor of the internal equipment forward of the engine, supplemental air from the cheater hole is required for optimum fan operation.

The model has the following dimensions:

Length	73 inches
Wing Span	47 inches
Mean Aerodynamic Chord	17.9 inches
Wing Reference Area	742.6 inches ^{2}
Aspect Ratio	2.97
Wing Leading Edge Sweep	40.1 $^\circ$
Weight	13.7 lbs

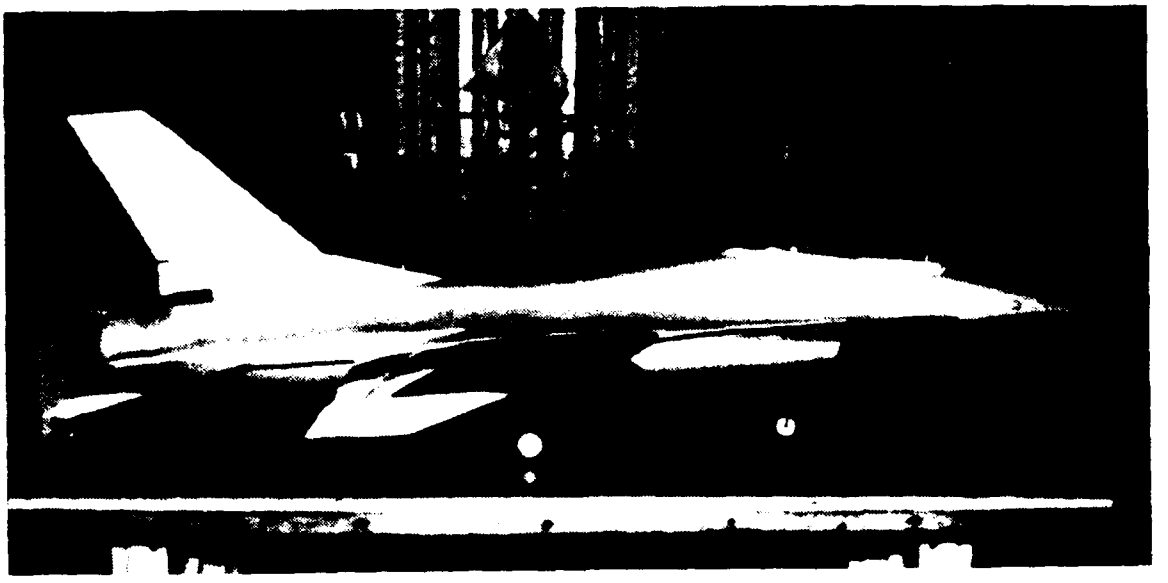

Figure 5. F-16A Model

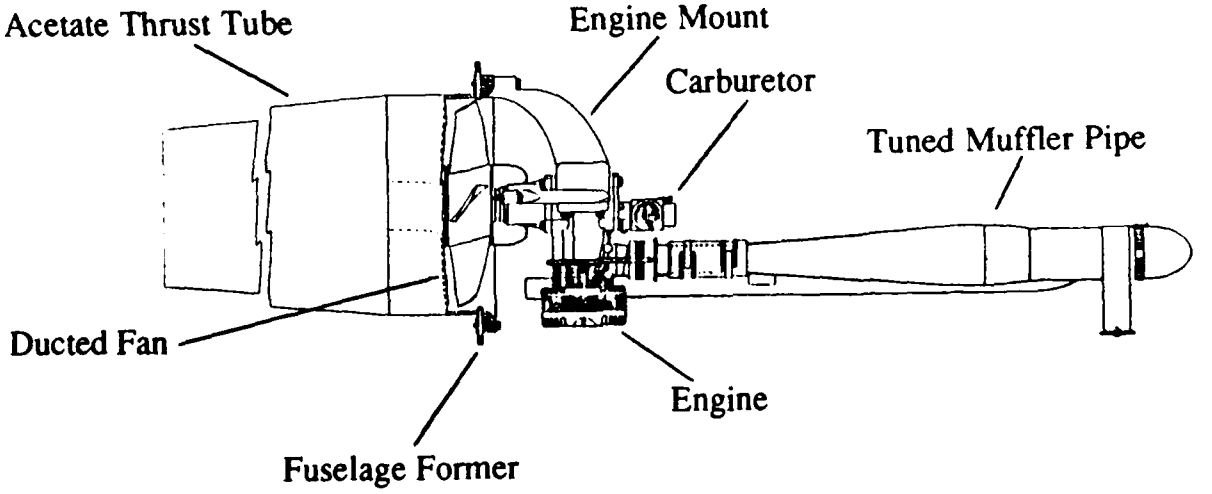

Figure 6. Engine-fan Assembly

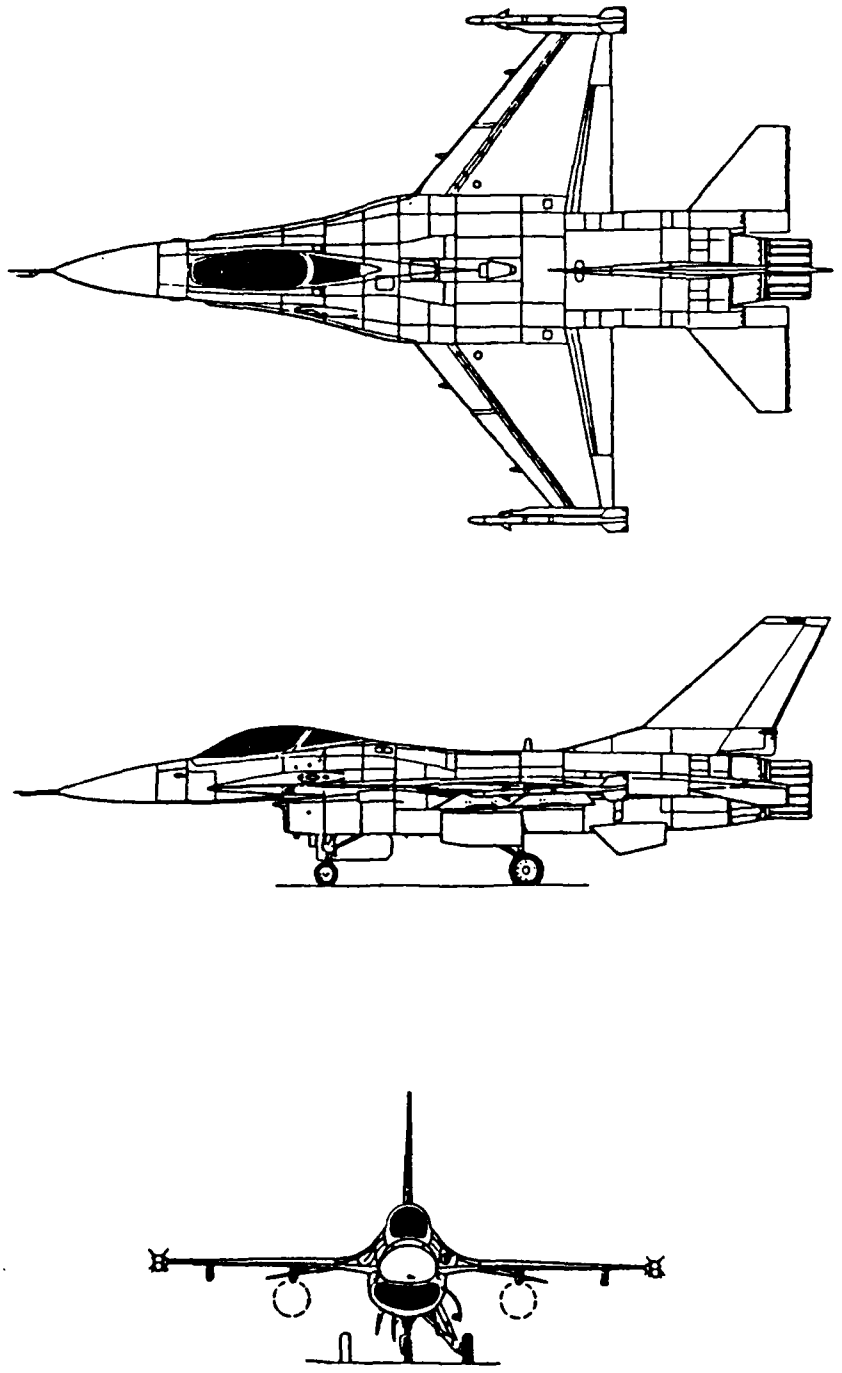

Figure 7. Three View Layout of F-16A (Full Scale)

The powerplant for the F-16A model consists of a Rossi™ .90 single piston engine with a displacement of 0.90 cubic inches. The engine is used to drive a six-inch diameter, five-bladed, ducted fan. A converging cylindrical acetate thrust tube, which extends to the exit nozzle, is used to minimize the flow turbulence aft of the fan housing due to the irregular shape of the fuselage. Additional flow acceleration is also achieved by means of the converging tube, resulting in a rated static thrust of 13.5 - 14.0 pounds at full power. A custom tuned muffler was designed such that the engine would rotate at a constant 20,400 RPM at full throttle, thereby attaining maximum thrust. The muffler system also provides pressurization for the fuel tank and for sound attenuation. Fuel is delivered to the engine through a venturi carburetor with two needle valves for controlling the fuel-air mixture: one for idle and the other for full throttle operation. Figure 6 shows the layout of the powerplant system.

The fuel system for the F-16A model consists of a 32-ounce fuel tank located on the upper side of the fuselage, on the aircraft longitudinal centerline. The aircraft is fueled through an external port on the right side of the fuselage. A fuel manifold is used to distribute the fuel during engine operation and ground refueling, depending on the status of a two position slide (aft for refueling and forward for engine operation). The fuel manifold is also used to route pressurization from the tuned muffler to the fuel tank.

A nine-channel radio control unit is used to maneuver the aircraft. In order to combat external noise and to increase the reliability of the signals, the digital proportional radio uses pulse code modulation (PCM). An analog signal (pilot input), passed through an analog-digital (A-D) converter, is encoded to an 8-bit digital word, and transmitted to the aircraft [Ref. 9:p 76]. The aircraft receiver

decodes the input, sends it to the respective servo which converts it to an analog signal. Consequently, only signals that are properly coded affect the aircraft. An incorporated fail-safe feature allows for the programming of the servos to any desired position in the event of signal loss (the F-16A model was programmed for neutral position for all control surfaces and 50% throttle). Servo motors are used to actuate flight controls, throttle, nose gear steering, and retractable landing gear. The servos are rated at 55.6 ounce-inches of torque with an operating speed of 0.24 sec/60°. A four-cell, 4.8 volt, 1200- milliamp battery pack provides the power for the aircraft receiver and servo group, while the hand-held transmitter utilizes a 9.6 volt, 500-milliamp battery pack. The transmitter has the programming flexibility to allow for adjustment of servo end point, servo response selection, flight control mixing, servo travel, and trim range.

B. ENGINE THRUST STAND

An engine thrust stand was constructed for measuring static thrust of ducted fan engines (Figure 8). The stand consisted of an engine-fan mount assembly, with thrust tube, which was attached to a platform slide designed with low friction bearings. A spring scale, calibrated from 0 - 20 pounds in 1/4 pound increments, was attached to the base of the test stand, which was in turn bolted to the test bench. The fuel supply was from a 24-ounce tank mounted on foam to reduce fuel foaming resulting from engine vibration. The thrust of the engine caused the platform slide to react opposite the thrust, thereby extending the spring scale.

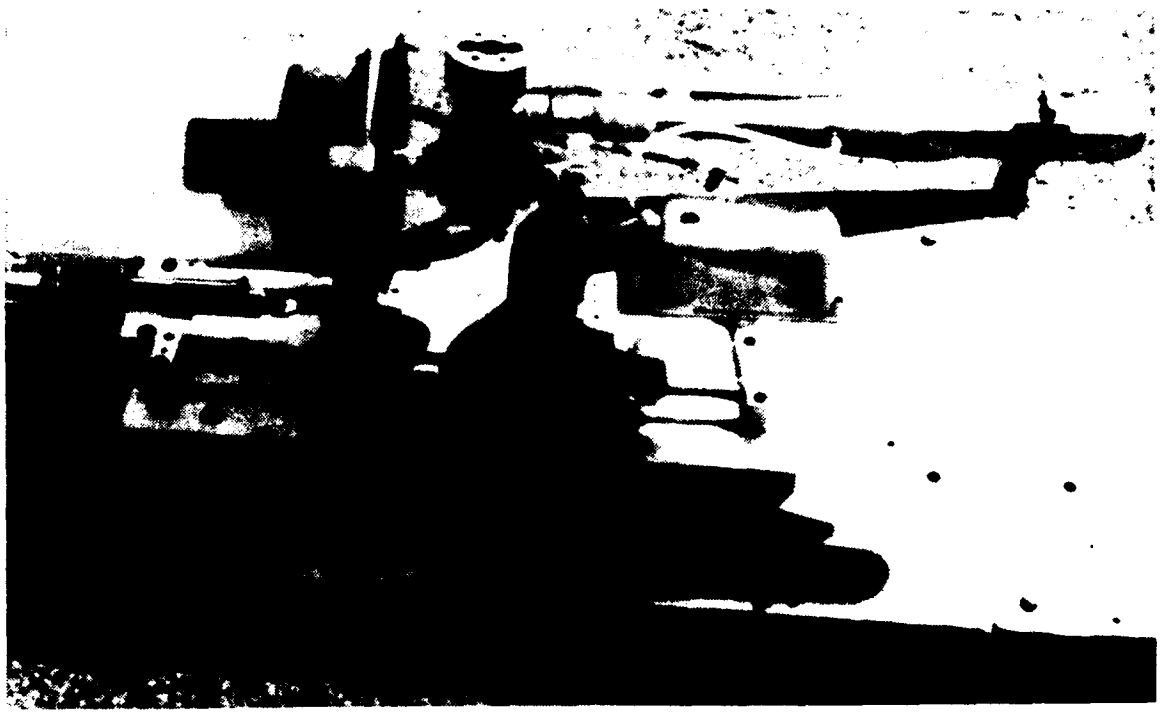

Figure 8. Engine Thrust Stand

C. WIND TUNNELS

1. NPS Vertical Wind Tunnel

The NPS vertical wind tunnel will be used to calibrate the alpha / beta vanes and airspeed indicator as a complete system. The calibration process will involve positioning the aircraft at various angle-of-attack and yaw combinations at slow speeds. The wind tunnel, shown in Figure 9, is a subsonic, single-return, closed-circuit type with a 3.5 x 5.0 foot octagonal test section. Though originally designed with two sets of counter-rotating fan blades, only the lower set existed due to damage and subsequent removal of the upper set. A 150-HP AC engine is used to drive the fan. The maximum speed in the test section with only one set of fan blades is 200 fps. The settling chamber will be used for the actual calibration process due to the small test section and large size of the model

and the resulting blockage factor. The contraction ratio of the tunnel is 6.84:1, which will give an approximate speed of 30 fps in the settling chamber. [Ref. 10:p. 11-14]

A 12-inch Prandtl tube will be used to measure the pressure differential in the settling chamber. The tube, connected to a digital manometer, will measure the pressure in inches of water. Bernoulli's equation will be used to determine the velocity of the flow.

2. NPS Horizontal Wind Tunnel

The horizontal wind tunnel was used for the initial calibration of the airspeed indicator, allowing for high speed and low speed data points. The wind tunnel, shown in Figure 10, was a subsonic, single-return, closed-circuit type with a 45 x 28.25 inch rectangular test section. Airflow was generated by a 100 HP electric motor coupled to a three-bladed constant-speed fan. Flow straighteners, located directly downstream from the fan blades, were designed to reduce the swirl generated by the blades. The flow continued through three sets of turning vanes before passing through turbulence reducing screens at the entrance of the settling chamber. An 11.42:1 contraction cone accelerated the flow to generate approximately 150 fps. The horizontal wind tunnel had a turbulence factor of 1.04. [Ref. 11:p. 11-13, 33]

A Prandtl tube connected to a digital manometer was again used to measure the pressure differential in the test section. The tube was located parallel to the airspeed indicator, at a transverse distance of three inches, in order to observe the same velocity without being affected by the propeller wash of the airspeed indicator. A digital frequency counter , connected directly to the

output leads, was used to measure the RPM of the airspeed indicator. An oscilloscope was also used to confirm the RPM frequency.

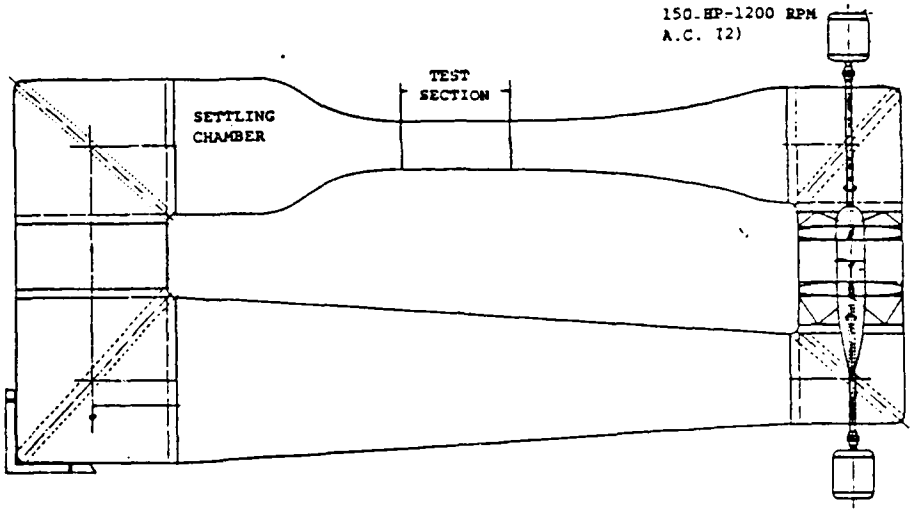

Figure 10. Vertical Wind Tunnel

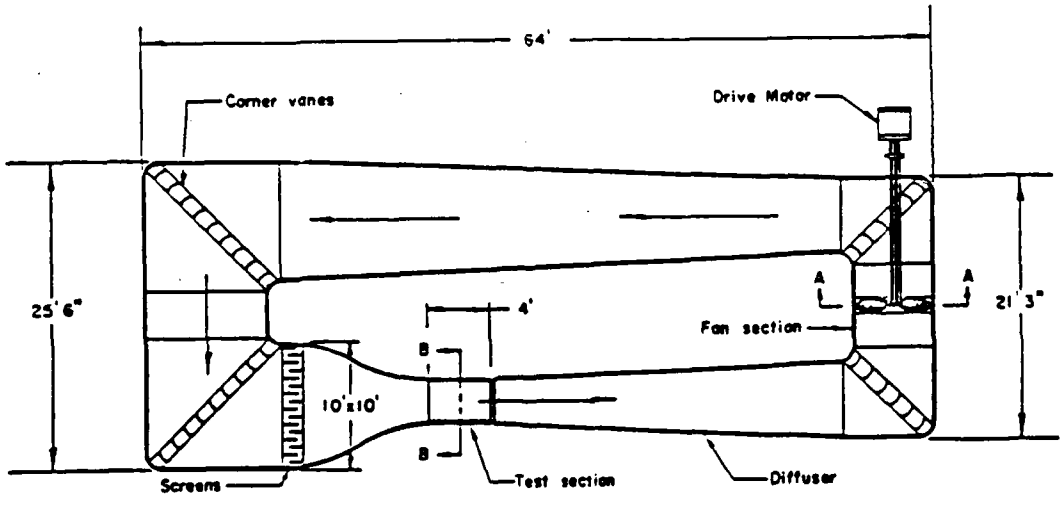

Figure 11. Horizontal Wind Tunnel

3. Small Scale Wind Tunnel

A small scale wind tunnel, shown in Figure 11, will be used for additional calibration of the airspeed indicator. The indicator will be connected to the circuit board that converts the pulse information provided by the CdS sensor to a voltage. The voltage output of the converter will be compared to the RPM of the indicator to determine airspeed. A detailed discussion of the airspeed converter circuit board is contained in the Telemetry Package section. The wind tunnel, developed at NPS, consists of a 6.5-feet long flow-through tunnel with a 5.0 x 5.0 inch square test section. A 1/3 horsepower motor drives a variable speed blower allowing a maximum speed of 50 fps.

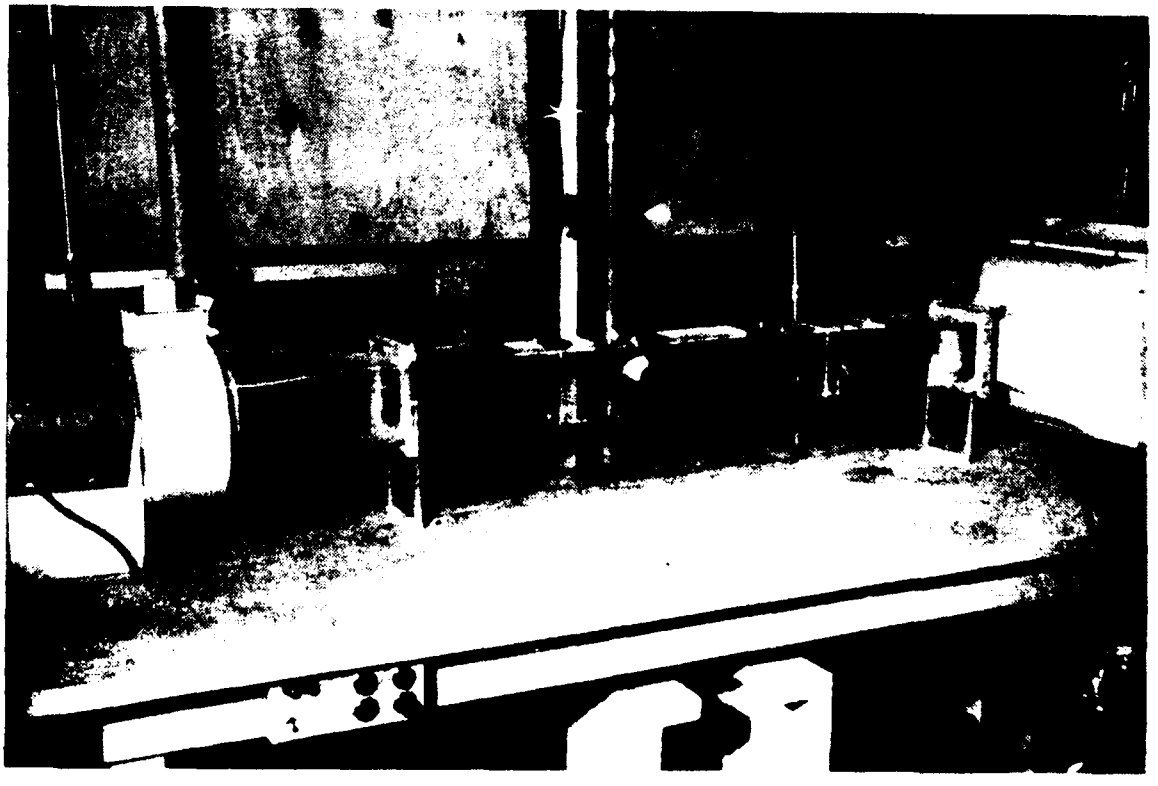

Figure 11. Small Scale Wind Tunnel

D. WIND TUNNEL TEST STAND

In order to calibrate the alpha and beta vanes and airspeed indicator as they will be configured on the aircraft, a test stand was designed for use in the settling chamber of the vertical wind tunnel (Figure 12). The rotating, circular base of the stand was constructed from 3/4-inch plywood and scaled from 0 - 12 degrees left and right of the longitudinal axis, in one degree increments, for generating sideslip angles (beta). The strut supports, made from prefabricated shelf supports and bolted to the rotating platform, were fixed to the aircraft at the landing gear attach points. The main landing gear were allowed to rotate by means of a bearing, and therefore had fixed length struts. The nose gear attach point was connected to an extendable strut which was calibrated in ten degree increments from -10 to +50 degrees angles of attack. During the proposed tests, the aircraft will be aligned with the longitudinal axis of the wind tunnel, facing the turning vanes at the entry of the contraction section.

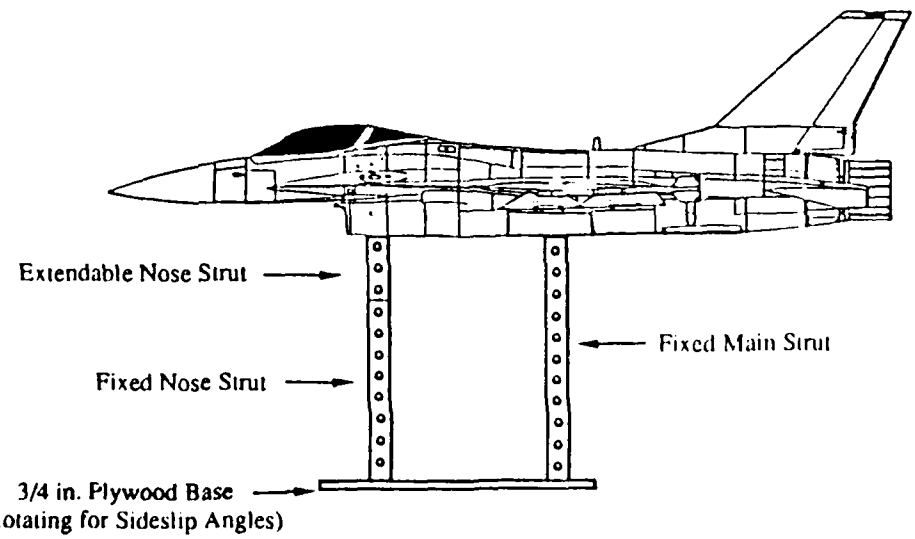

Figure 12. Vertical Wind Tunnel Test Stand

The information from the aircraft sensors will be transmitted to the telemetry ground station for calibration.

E. TELEMETRY PACKAGE

The telemetry package consists of an encoder/transmitter set, a bank of operational amplifiers for the encoder/transmitter, an airspeed indicator frequency-to-voltage conversion circuit, a set of low torque potentiometers for alpha and beta measurements, a 9.6-volt battery pack for the encoder/transmitter, and a 4.8 volt battery pack for the alpha and beta potentiometers. The ground based receiver consists of a standard radio control receiver powered by a 4.8-volt battery pack and connected to servos in order to generate analog voltages.

1. Encoder/Transmitter and Operational Amplifier Bank

A seven-channel encoder/transmitter set, operating at a frequency of 27.192 MHz, will be used to transmit the flight parameters to the ground based receiver. Voltage output from the control surface servos will be connected to the operational amplifiers (op-amps) in order to ensure a sufficient voltage for transmission (see Figure 13). The integrated circuit (IC) chip used is a LM1458, with two op-amps per chip, designed to increase the input by a factor of 2. All channels will be routed through the op-amp circuit with the exception of the battery voltage reference. The battery voltage maintains a relatively high signal strength and does not requires a signal boost.

The encoder section will utilize analog voltage inputs from the aircraft sensors. In order to help minimize electro-magnetic interference (EMI) inherent in this system (between the aircraft receiver control group and telemetry transmitter), twisted-pair shielded wire will be used for connections running the length of the fuselage. Shorter lengths will not contribute greatly to the EMI

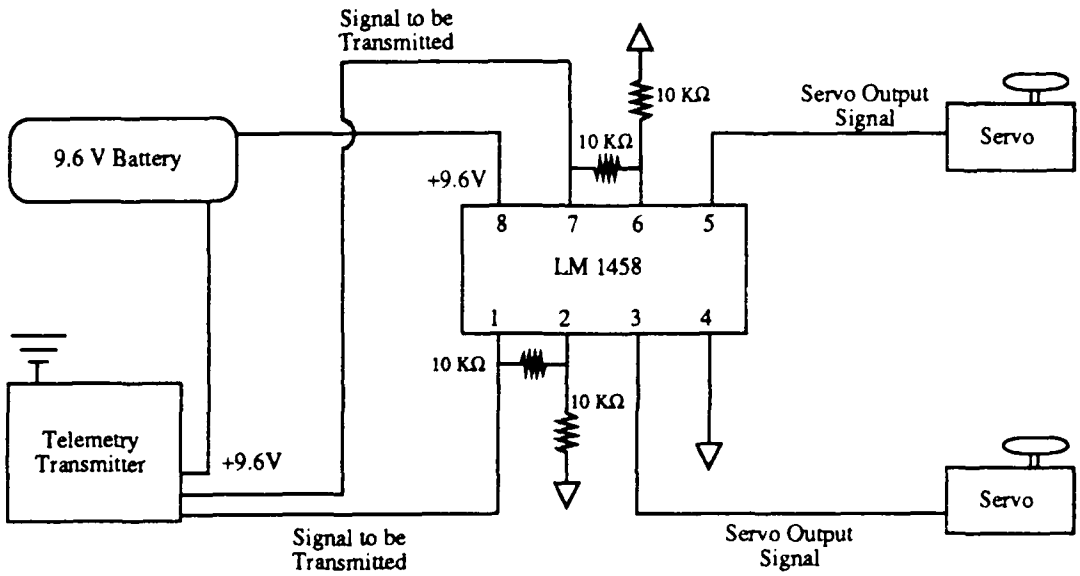

Figure 13. Operational Amplifier Circuit

problem. All input leads to the actual encoder IC board will be routed through ferrite beads, which act as inductors, thereby helping reduce the effects of EMI. Capacitors, rated at .01 μf, will also be connected between the channel inputs and ground to act as low pass filters. The encoder converts the analog signal to a pulse width, which is modulated according to the level of input voltage. The pulse width will be transmitted by the radio frequency (RF) transmitter deck to the ground based receiver. The receiver decodes the signal and sends it to the designated servo where it will be converted back to an analog signal. The results will then be displayed on an ammeter, and recorded by a seven-channel data recorder.

2. Airspeed Indicator

The airspeed sensor, shown in Figure 14, receives its input from a CdS photo sensor which monitors the RPM of the propeller. The CdS sensor operates by sensing the light level and changing its resistance according to the passing of

light "blockers" on the rear of the propeller. The net result, when connected with a 4.8-volt power supply, is a sinusoidal waveform that has a shorter period with increasing RPM (or airspeed). The input passes through a series of voltage dividers and enters a LM311 voltage comparator. The comparator senses the positive slope region of the sinusoidal waveform and triggers a "high" condition of 5.0 volts. Conversely, the negative slope portion triggers a "low" condition of 0.0 volts. The resulting output is a square waveform whose period correlates with the sinusoidal waveform. However, the average of this output is always 2.5 volts, which is of no use in determining airspeed. A 7555 timing chip utilizes the "sharp" square waveform (highs and lows) to generate a waveform with a constant pulse width and magnitude, regardless of the airspeed. The number of pulse widths within a given time interval will vary with airspeed; therefore, the average of the constant pulse widths within that interval result in a voltage output that changes with changing airspeed.

A time constant is calculated to determine the maximum pulse width of the signal generated by the 7555 chip. The time constant, in turn, determines the correct resistor-capacitor (RC) combination utilized by the 7555 chip. During the airspeed indicator calibration process, a frequency of 140 Hz was determined to be the maximum for the experiment. In general, the maximum pulse width generated by the 7555 chip should be equal to no more than the period of the maximum frequency. The desired RC combination is calculated using equation (1):

$$2/3 = e^{-t/RC} \qquad (1)$$

Solving for RC, with the time constant $t = 1/f = 1/140$, and a capacitance of

0.05 µf, the resistance required is 360 KΩ. Figure 15 depicts the airspeed frequency-to-voltage conversion circuit.

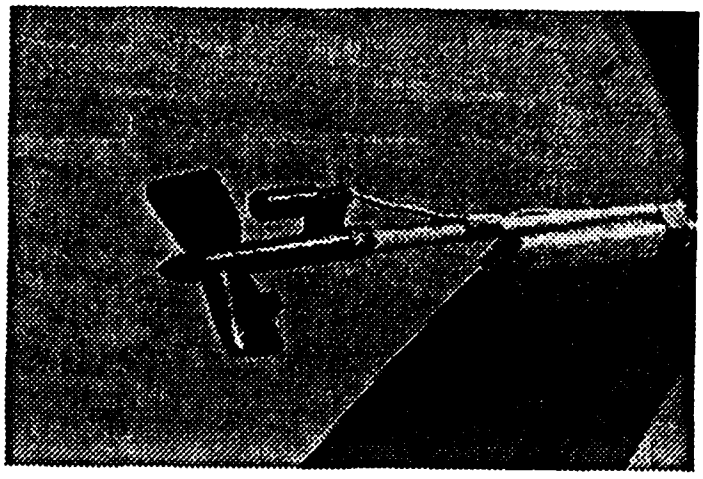

Figure 14. Airspeed Sensor

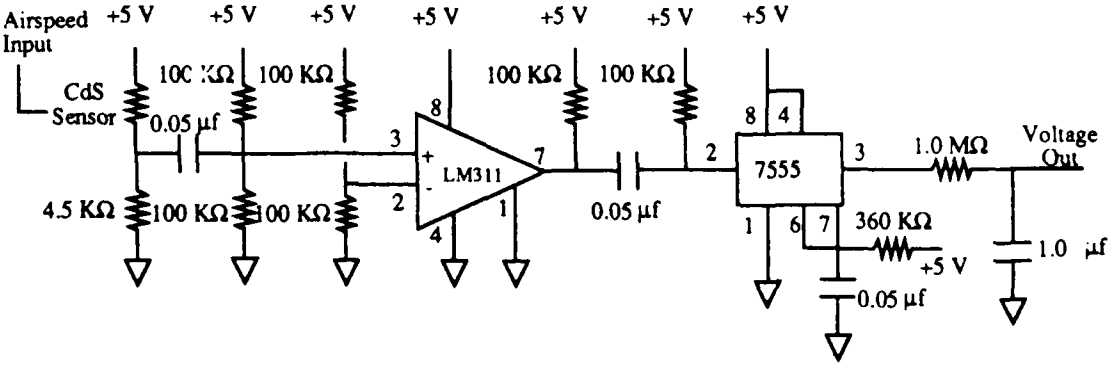

Figure 15. Airspeed Frequency-to-Voltage Conversion Circuit

3. Alpha and Beta Vanes

The alpha and beta vanes were constructed from 1/8-inch brass tubing and 1/32-inch brass sheeting. The connecting shaft and fin were soldered to the

vane shaft (see Figure 16). The vanes were connected to low-torque potentiometers by a 1/4-inch diameter aluminum rod, with set screws to hold the vanes in place. The potentiometers weighed 0.6-ounces, and were rated at 0.25 inch-ounces of torque. The potentiometers will receive power from a 4.8-volt battery pack, and be connected to the op-amp circuit.

In order to ensure accurate angle-of-attack determination during sideslip conditions, two vanes are used, extending approximately 1.75 inches from each side of the forebody. The yaw vane extends approximately 1.5 inches below the nose, on the longitudinal axis of the aircraft.

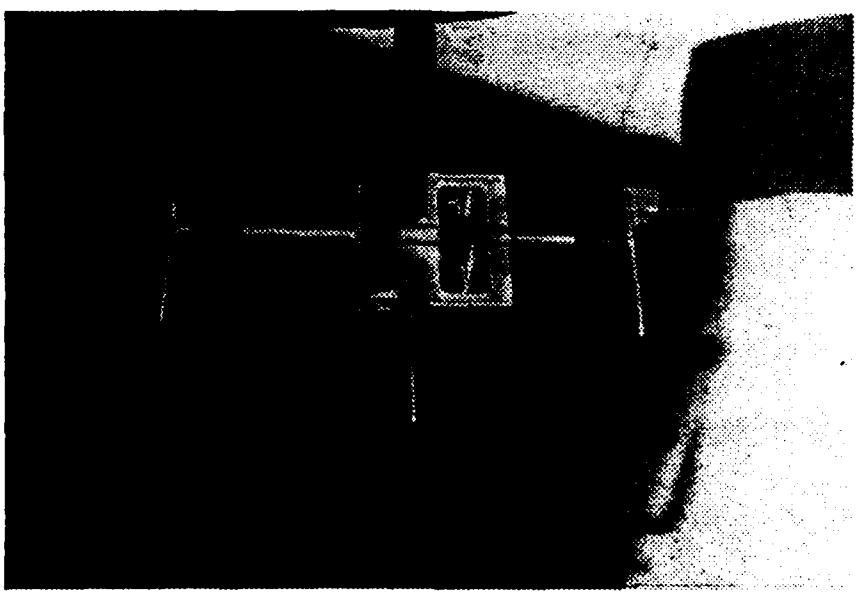

Figure 16. Alpha/Beta Vanes

4. Ground Station

The ground station will includes a seven-channel receiver (decoder), seven analog meters for real time output and video recording, and a seven-

channel data recorder. Signals received from the telemetry encoder/transmitter in the aircraft will be decoded, passed to designated channels, and converted to an analog voltage. Servos, with leads attached to the potentiometers, will be used to convert the signal to an analog voltage. The voltages from the servo potentiometers will be output through a "Y" connector to the analog meters and data-recorder.

IV. EXPERIMENTAL PROCEDURE

A. ENGINE BREAK-IN

The Rossi™ .90 engine was initially disassembled and cleaned, and the piston and cylinder case sanded with 600-grit emory cloth in order to remove any burrs. The piston top edge was chamfered 0.01 inches to ensure no catastrophic interaction between the edge and sharp exhaust port edges during thermal expansion. The first four runs were made using a rich fuel-air mixture to keep the engine from overheating. A tractor propeller was also used to keep a continuous airflow over the cylinder head to aid in cooling. Throttle settings ranged from idle to full-power, with the tuned muffler pipe set at a position that limited the RPM at full throttle. The last two runs were made with the tuned muffler pipe set at the manufacturer's suggested position for maximum obtainable RPM. The idle and full throttle needle valves were set at the optimum fuel-air mixture at the low and high end.

The tractor propeller was removed and the six-inch fan attached. The unit was mounted to the engine thrust stand for static thrust tests. Due to lack of airflow over the cylinder head provided by the fan, high throttle settings were limited to approximately 20 seconds. The engine was then shut down and allowed to cool. A white timing stripe was painted on the fan to allow for RPM determination with a hand-held sensor. During the test runs, the tuned muffler pipe was positioned for maximum RPM at full throttle as determined during the break-in. The fuel-air mixture was set during the high speed run to allow for maximum RPM as well. Due to the sensitivity of the engine to fuel-air mixture at high RPM, and the limited time available to achieve the correct setting, the

indicated thrust varied ± 0.75 pounds. Table 2 lists the results of the two runs. The second run did not have the optimum high end fuel-air mixture set and therefore indicated a slightly lower thrust.

TABLE 2. STATIC THRUST TEST RESULTS

Run	RPM	Maximum Thrust	Average Thrust
1	19,700	13.5 lbs.	12.50 lbs.
2	19,900	13.0 lbs.	12.25 lbs.

B. AIRSPEED CALIBRATION

The calibration of the airspeed indicator involved three separate steps. The first calibration process consisted of verifying that the digital counter used to indicate frequency corresponded to the actual frequency of the airspeed indicator. An oscilloscope was connected directly to the output terminals of the indicator. The frequency on the oscilloscope indicated two times the actual frequency because of the light blockers on each of the propeller blades. The digital frequency counter was connected to the output of the 7555 timing chip, and counted the number of pulses, from which the frequency was determined. Both signals were in agreement. The small scale wind tunnel was used for this process.

The second calibration, conducted in the horizontal wind tunnel, consisted of plotting the frequency of the indicator versus the flow velocity (derived from the measured pressure differential). The indicator was placed near the center of the test section, parallel to the Prandtl tube. The digital manometer, scaled in inches

of water, was initialized to zero at the start of each run, and at three minute intervals to limit any drift in the manometer system. Two runs were made in order to ensure repeatable data. Bernoulli's equation, Equation (2), was used to compute the velocity of the flow.

$$V_{fps} = \sqrt{(2 * \Delta P)/(\rho/g_c)} \qquad (2)$$

The data points from each run, listed in Appendix A,Table 3, were plotted together, and a linear regression performed to test for linearity (see Figure 17). With the exception of the data points at 58 Hz and 119 Hz, the airspeed indicator responded in a linear manner. The 58 Hz data point was near the low end of the sensitivity range, and may have been an erroneous point due to the low end resolution of the airspeed indicator. The source of error in the 119 Hz data point was undeterminable. Excellent linearity existed in the region from 26 to 46 MPH, which corresponds to the estimated stall speed of the model.

C. FLIGHT TEST

The initial flight tests were conducted in order to evaluate the basic flight characteristics of the aircraft. The telemetry system was not installed in the aircraft. The transmitter and receiver batteries were allowed to charge overnight to allow for as many flights as possible the following day. The flight tests were conducted at the Salinas Area Modelers Airfield, which consisted of an approximate 375 x 50 foot paved asphalt runway.

Prior to flight, all control surface linkages and connections were checked to ensure proper operation and integrity. A ground test of the transmitter was conducted by moving away from the aircraft with the transmitter antenna in the

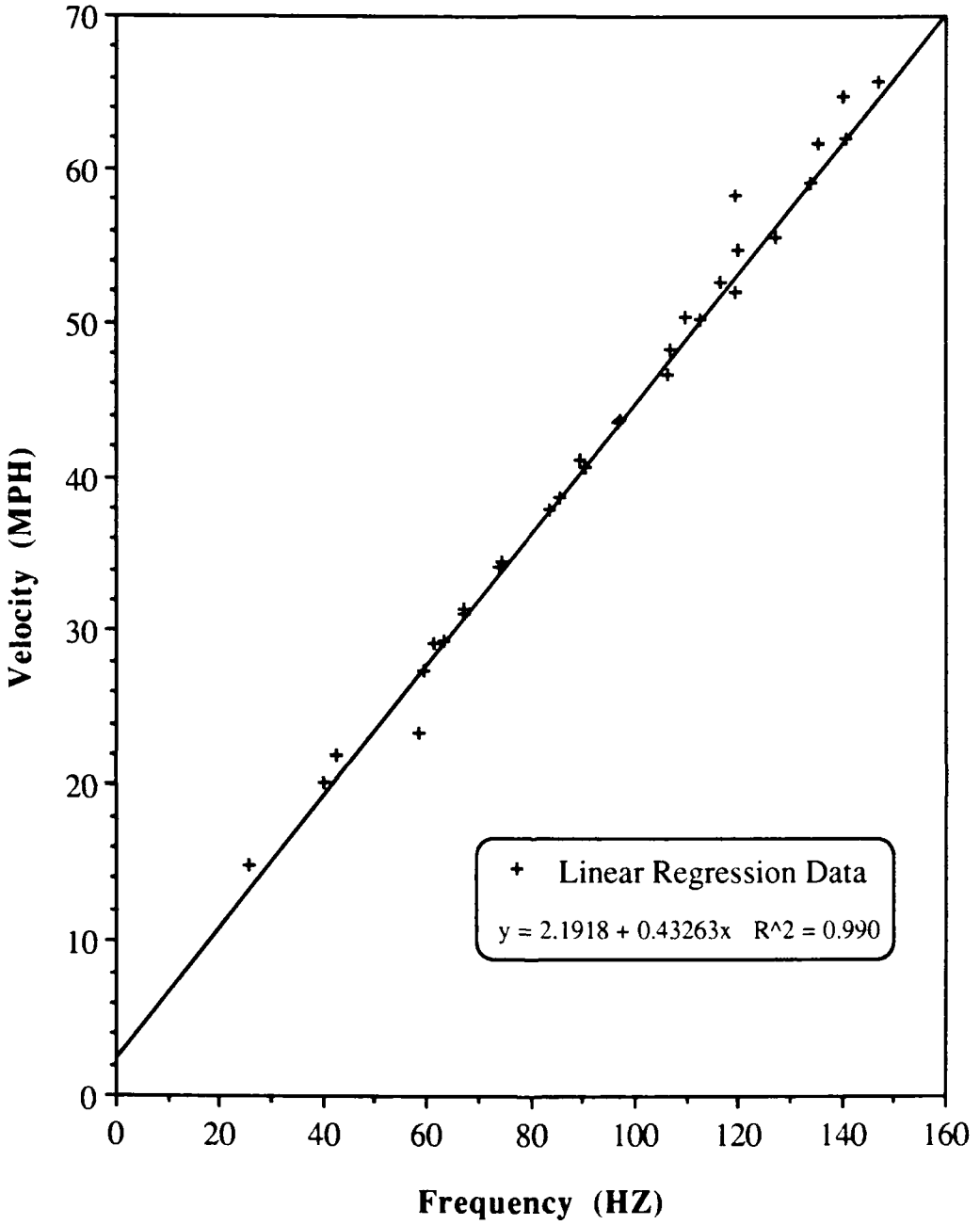

Figure 17. Airspeed Indicator Calibration

retracted position, and observing flight control movement. Flight control movement corresponded to pilot input up to a distance of approximately 100 feet.

The center of gravity (CG) was determined by using a force-moment arm method. The total weight of the aircraft without the telemetry equipment was 12.06 lbs., with 1.65 lbs. (13.68%) distributed on the nose landing gear and 10.41 lbs. (86.32%) distributed on the main landing gear. With a distance of 18.56 inches between the nose and main gear, the center of gravity was calculated at 2.54 inches forward of the main gear. The main gear were positioned 0.75 inches forward of the engine former, therefore, the center of gravity was located slightly aft of the manufacturer's suggested location of 3.5 inches forward of the former (22% MAC).

The engine was started by means of a 3-foot starter "wand" connected to a high-torque starter. The wand was inserted up the tailpipe and engaged the ducted fan retainer nut. The wand had a clutch that allowed the starter socket to turn in only one direction, thereby avoiding unintentional loosening of the nut. For engine start, the glow plug received its power from a 1.5-volt power supply. Once the engine was running, the test pilot adjusted the mixture at both high power and idle by listening to the sound of the engine. A trace of white smoke was also an indication of a proper mixture at full power. A ground taxi test was conducted to ensure controllability on the ground.

The objective of the first flight was to determine the basic handling characteristics of the aircraft, and to trim for "hands-off" straight and level flight conditions. After takeoff the gear was retracted and a right-hand racetrack pattern established. The flight was conducted at a relatively high power setting,

therefore, a timer was set for three minutes to allow sufficient fuel for a powered landing. The second and third flights consisted of further refinement of the engine fuel-air mixture at higher power settings and basic flight handling. A level pass at approximately 20° angle of attack was made on the third flight to demonstrate the low speed capability of the the aircraft.

The telemetry package was not installed on subsequent flights due to technical problems encountered in the ground output signal. Further discussion of the problems is included in the Results section.

V. RESULTS AND RECOMMENDATIONS

A. RESULTS

1. Flight Test

Ground handling characteristics were evaluated during low power taxi tests. Though ground handling characteristics were acceptable, the aircraft responded abruptly to small steering inputs, making exact control difficult. Numerous small inputs were required to maintain proper tracking. The nose wheel angular deflection per unit control input was reduced by approximately 25% to allow for smoother ground handling and more precise tracking. Figure 18 shows a nose wheel response gradient, with breakout occuring at approximately 8%.

The longitudinal control characteristics of the aircraft were excellent. The aircraft required only minor nose-up trim for level flight. The aircraft was fully controllable with the available stabilator control deflection (9.0° leading edge up, 9.0° leading edge down) over the full range of flight test airspeeds. No significant pitch changes were noted with power addition/reduction, or with landing gear extension/retraction. Stabilator control authority at low speeds (landing pattern) was adequate. Figure 19 shows the stabilator response gradient.

Lateral controllability was also excellent, requiring only minor right wing down trim to maintain balanced flight. Roll rate was examined on three aileron rolls, two with intermediate deflection and one with full deflection. Roll rate was crisp and no adverse yaw tendencies were noted. Lateral control power

was sufficient to correct for gust-induced rolls encountered during low speed approaches to landing. Roll control was evaluated at two aileron deflection

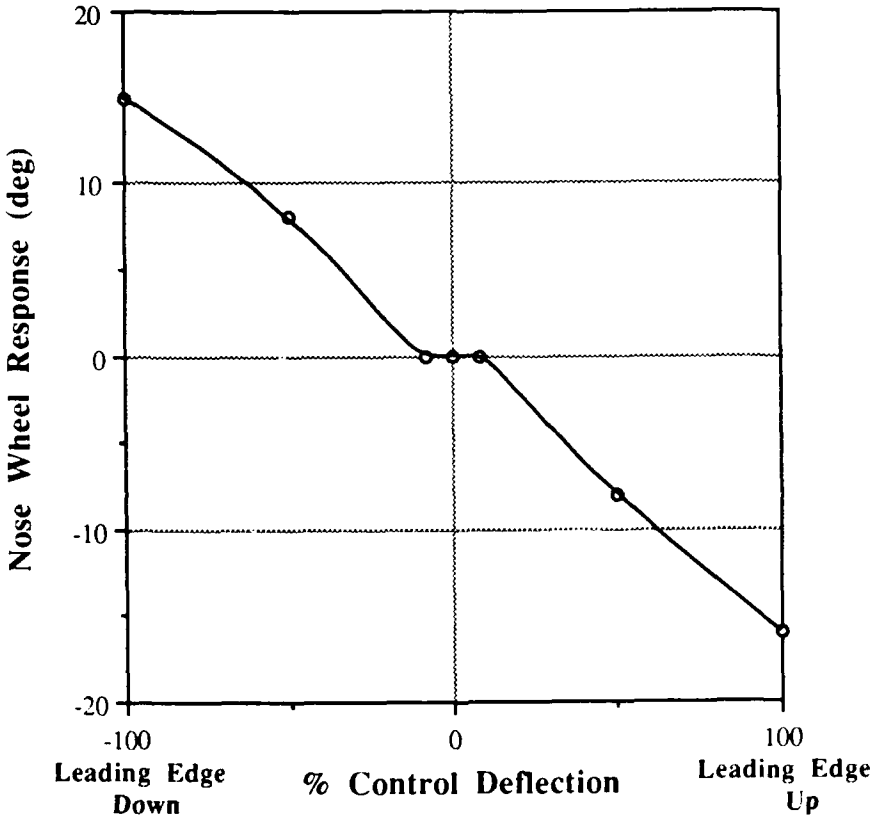

Figure 18. Nose Wheel Response versus % Control Deflection

limits. Configuration A-1 limited deflection to ± 20.6° and A-2 limited deflection to 17.2°. Roll rate with A-1 was very quick and required little stick movement for a given rate, which could create a tendency to over-control lateral inputs. A-2 reduced the roll rate for a given stick input, which made roll-angle capture more precise. Figure 20 shows the aileron response gradient.

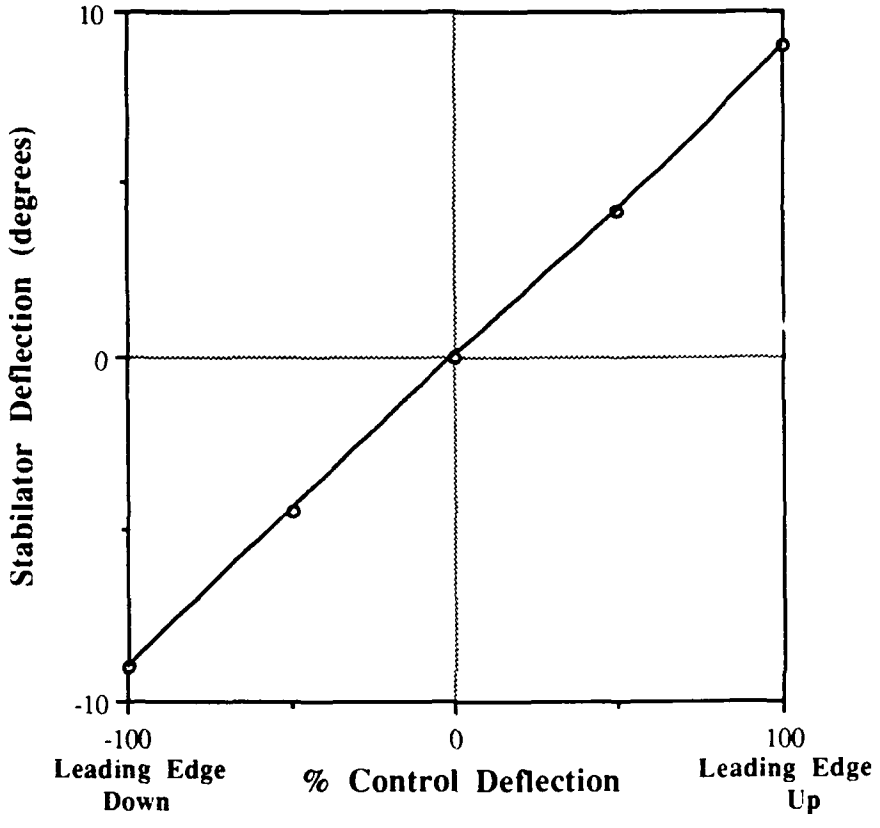

Figure 19. Stabilator Response versus % Control Deflection

The ducted fan provided sufficient power for the aircraft through the tested flight envelope. Takeoff roll was 175 feet, with an approximate 30° climb angle after takeoff. The power setting used during the test flight was virtually full power. There was no significant spool-up time encountered with the engine-fan system as demonstrated during idle-to-full power throttle bursts. The second landing attempt resulted in a high sink rate which caused the aircraft to bounce approximately four feet back into the air. Controllability was regained and a successful wave off accomplished when full power was applied. Due to the

limited scope of the flight tests, minimum control speed and maximum level flight speed were not determined.

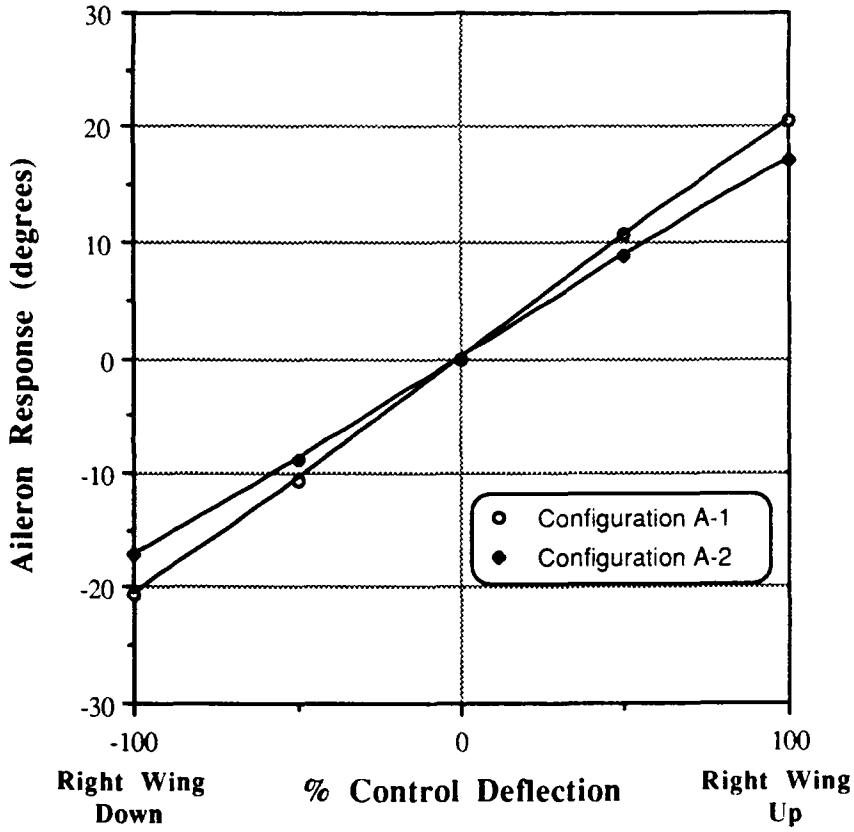

Figure 20. Aileron Response versus % Control Deflection

2. Telemetry System

The telemetry system was tested using an analog output voltage from a servo potentiometer connected to the aileron channel. Nominal voltage output was 1.27 volts for the neutral position. Full stick deflection in both directions

resulted in an equal and linear increase/decrease in voltage output. The op-amps functioned properly by increasing the servo output voltage by a factor of two. However, technical problems with the input signal to the encoder/transmitter prevented the system from becoming fully operational for flight tests.

When originally designed, a potentiometer was connected directly to the encoder/transmitter circuit board to simulate a voltage input from a control servo (or other flight measurement source). The potentiometer received it's power from the encoder board, and therefore had the correct centerpoint voltage since it was determined by the on-board circuitry. Output from the ground station receiver was equal and linear in both directions. However, inputs from the aircraft servos, alpha/beta vanes, and airspeed circuit used external power sources. Each of the inputs had different centerpoint voltages, which in turn were offset from the centerpoint voltage expected by the encoder. The result was an asymmetrical analog voltage output by the ground station. With full stick aileron deflection to the right, the ground station output 0.38 volts above the neutral voltage, but full stick aileron deflection to the left output only 0.08 volts below neutral voltage. Other channels produced the same asymmetric characteristics.

Another anomaly occurred when multiple channels were connected. Output from the ground station receiver seemed to decrease when more than one channel was receiving data. With the aileron and stabilator channels connected, output voltage decreased approximately 25%. The source of this problem was not determined.

B. RECOMMENDATIONS

1. Flight Test

The deficiency in the telemetry package precluded calibration of the flight performance measurement systems. Once the deficiency is corrected and a fully operational package is available, a static (flight control deflections) and dynamic (alpha/beta vanes and airspeed indicator) calibration process will be required.

The 1/8-scale F-16A is expected to be an excellent test-bed for supermaneuverability studies. The general stability and control of the aircraft was excellent with the CG located at 22% MAC. Flight data are required in the standard configuration to establish a baseline for performance comparison, prior to any airframe modifications. Follow-on flight test should include determination of the aft CG limit in order to allow for maximum maneuverability. Methods of increasing stabilator deflection should also be investigated for creating higher pitching moments, especially for controllability reasons at high angles of attack.

Evaluation of the external sensors should be evaluated for optimum location. The airspeed indicator may have potential wake turbulence or fuselage blockage problems at high angles of attack, which would provide inaccurate performance data.

Initial configuration changes should be limited to moderate airframe changes, such as a strake modification, or addition of the fixed strakes on the forebody. The flight control mixing capability of the radio-control transmitter will permit integration of control surface deflection, such as flaps extension combined with normal stabilator movement for pitch authority.

2. Telemetry System

The first goal of follow-on work needs to be resolution of the telemetry system deficiency. A bias circuit needs to be designed for use by each sensor, allowing for individual adjustment. This will aid in eliminating the differential voltage centerpoints between the encoder and sensors. An in-house circuit board also needs to be designed/evaluated for converting the transmitted signal to an analog voltage, other than through another servo decoder. A circuit board designed by Dr. James Hauser is available, but has yet to be tested. A potential source for electronic design support is Mr. Tom Christian, an electronics technician attached to the Mechanical Engineering Department an the Naval Postgraduate School. His design of a telemetry system for an underwater research vehicle may be expanded to incorporate UAV applications.

The seven-channel telemetry system is somewhat limited for dynamic flight measurements. A 14-channel system would allow measurement of more flight parameters, thereby providing additional performance evaluation data. A method of accomplishing this task would be to multiplex the current seven-channel system. A disadvantage of this method would be a decrease in sampling rate by half (from 60 Hz to 30 Hz). However, certain parameters would not necessarily require a high sampling rate (flight control deflection for example). This would allow for measurement of accelerations (pitch/roll/yaw), altitude, and throttle setting, all of which are desirable data points. With the above system, a method of recording the increased number of channels would have to be developed, or multiple flights would have to be made under similar flight conditions to record the additional data. In addition, a new circuit design would be necessary.

With the limited amount of space available for radio-control/telemetry equipment, miniaturization is an important consideration. Alternatives to current equipment must be continuously evaluated. The added benefit of miniaturization is the associated weight savings. One example is the miniature potentiometers utilized by the Naval Research Laboratory in their UAV research.

APPENDIX A. RAW DATA TABLES

TABLE 3. AIRSPEED CALIBRATION DATA

Run 1				
Wind Tunnel ΔP		Velocity	Velocity	Frequency
In. Water	psf	fps	mph	Hz
0.38	1.98	40.68	27.73	55.30
0.47	2.45	45.30	30.89	61.20
0.60	3.12	51.11	34.85	69.30
0.68	3.54	54.42	37.10	74.80
0.78	4.06	58.36	39.79	80.30
0.85	4.42	60.92	41.54	83.90
0.91	4.73	63.04	42.98	89.50
1.09	5.67	68.89	46.97	97.50
1.26	6.56	74.07	50.50	105.70
1.41	7.34	78.36	53.42	112.40
Run 2				
Wind Tunnel ΔP		Velocity	Velocity	Frequency
In. Water	psf	fps	mph	Hz
0.24	1.25	32.33	22.04	42.70
0.43	2.24	43.27	29.50	63.50
0.49	2.55	46.19	31.49	67.00
0.59	3.07	50.69	34.56	74.60
0.71	3.69	55.60	37.91	83.50
0.82	4.27	59.75	40.74	90.50
0.95	4.94	64.32	43.85	97.30
1.08	5.62	68.58	46.76	106.40
1.25	6.50	73.78	50.30	112.50
1.34	6.97	76.39	52.08	119.20
1.53	7.96	81.62	55.65	127.30
1.73	9.00	86.79	59.18	133.70
1.90	9.88	90.96	62.02	140.50
2.14	11.13	96.53	65.82	147.00
Temperature:		59 ° F	(518.67 ° R)	
Barometric Pressure:		30.05 in Hg	(2125.35 psf)	
Gas Constant:		53.30	ft-lbf/lbm-°R	
Density (local):		0.0769	lbm / ft^3	

TABLE 4. CONTROL RESPONSE DATA

Nose Wheel Steering

Deflection (%)	Direction (Left/Right)	Amount (Degrees)
1.0	Left	15.0
0.5	Left	8.0
0.0	Center	0.0
0.5	Right	8.0
1.0	Right	16.0

Breakout: ± 8.0 %

Stabilator Response

Deflection (%)	Direction (L.E. Up/Down)	Amount (Inches)
1.0	Down	0.75
0.5	Down	0.37
0.0	Neutral	0.00
0.5	Up	0.35
1.0	Up	0.70

Breakout: ± 0.0 %

Aileron Response Response

Deflection (%)	Direction (R.W. Up/Down)	A-1 Amount (Inches)	A-2 Amount (Inches)
1.0	Down	0.75	0.62
0.5	Down	0.37	0.31
0.0	Neutral	0.00	0.00
0.5	Up	0.37	0.31
1.0	Up	.75.	0.62

Breakout: ± 0.0 %

LIST OF REFERENCES

1. Dorn, M.D., *Aircraft Agility: The Science and the Opportunities*, AIAA Paper 89-2015, August 1989.

2. Gilbert, W.P., Nguyen, L.T., and Gera, J., *Control Research in the NASA High-Alpha Technology Program*, AGARD Symposium Paper, October 1989.

3. Herbst, W.B., *Future Fighter Technologies*, Journal of Aircraft, Vol. 17, No. 8, August 1980.

4. Reznick, S.G. and Flores, J., *Strake-Generated Vortex Interactions for a Fighter-Like Configuration*, Journal of Aircraft, Vol. 26, No. 4, April 1989.

5. Murri, D.G. and Rao, D.M., *Exploratory Studies of Actuated Forebody Strakes for Yaw Control at High Angles of Attack*, AIAA Paper 87-2557, 1987.

6. Deets, D.A. and Brown, L.E., Experience with HiMAT Remotely Piloted Research Vehicle - An Alternate Flight Test Approach, AIAA Paper 86-2754, October 1986.

7. Hollerman, E., NASA Technical Note D-8052, *Summary of Flight Tests to Determine the Spin and Controllability Characteristics of a Remotely Piloted, Large Scale (3/8) Fighter Airplane Model*, January 1976.

8. Raney, D.L. and Batterson, J.G., NASA Technical Memorandum 4108, *Lateral Stability Analysis for X-29A Drop Model Using System Identification Methodology*, March 1980.

9. Rosner, R.D., *Satellites, Packets, and Distributed Telecommunications*, Wadsworth, Inc., 1984.

10. Tanner, J.C., *Development of a Flight Test Methodology for a U.S. Navy Half-Scale Unmanned Air Vehicle*, Master's Thesis, Naval Postgraduate School, March 1989.

11. Department of Aeronautics and Astronautics, *NPS Laboratory Manual for Low Speed Wind Tunnel Testing*, Naval Postgraduate School, August 1989.

12. Lacey, D.W., *Aerodynamic Characteristics of the Close Coupled Canard as Applied to Low-to-Moderate Swept Wings, Volume 2: Subsonic Speed Regime*, David W. Taylor Naval Ship Research and Development Center Report, January 1979.

INITIAL DISTRIBUTION LIST

	No. Copies
1. Defense Technical Information Center Cameron Station Alexandria, VA 22304-6145	2
2. Library, Code 0142 Naval Postgraduate School Monterey, CA 93943-5002	2
3. Chairman, Code 67 Department of Aeronautics and Astronautics Naval Postgraduate School Monterey, CA. 93953-5000	2
4. Professor Richard M. Howard, Code 67Ho Department of Aeronautics and Astronautics Naval Postgraduate School Monterey, CA. 93953-5000	7
5. Lcdr Chris Cleaver 1501 Crystal Drive, Apt. 1034 Arlington, VA 22202	2
6. Academy of Model Aeronautics 1810 Samual Morse Drive Reston, VA 22090	1
7. Mr Richard J. Foch Naval Research Laboratory Code 5712 4555 Overlook Avenue, S.W. Washington, D.C. 20374	1
8. Dr. James P. Hauser P.O. Box 3021 Boulder, CO 80307	1

9. Thomas Momiyama — 2
Benjy Neumann
Naval Air Systems Command
AIR-931K
Washington, D.C. 20361

10. David W. Lewis — 1
UAV-JPO
Code PDA-14UD1D
Washington, D.C. 20361-1014

11. William C. Lindsay — 1
WRDC/FIGL
Wright-Patterson AFB, OH 45433-6503

12. Don Meeks — 1
1044 John Street, #40
Salinas, CA 93905

13. Mike Callaway — 1
3245 Tenley Drive
San Jose, CA 95148